Carbon
Volume 50, Issue 3, March 2012, Pages 845-850

doi:10.1016/j.carbon.2011.09.043 | How to Cite or Link Using DOI
Permissions & Reprints

Field emission of ribonucleic acid–carbon nanotube films prepared by electrophoretic deposition

Yang Doo Lee[a], Woo-Sung Cho[a], Yong Churl Kim[b], Byeong-Kwon Ju[a]

CARBON 50 (2012) 845–850

Available at www.sciencedirect.com

SciVerse ScienceDirect

journal homepage: www.elsevier.com/locate/carbon

Field emission of ribonucleic acid–carbon nanotube films prepared by electrophoretic deposition

Yang Doo Lee [a], Woo-Sung Cho [a], Yong Churl Kim [b], Byeong-Kwon Ju [a,*]

[a] Display and Nanosystem Lab., College of Engineering, Korea University, Anam-dong, Seongbuk-gu, Seoul 136-713, Republic of Korea
[b] Display Devices and Processing Lab., Samsung Advanced Institute of Technology, Giheung-gu, Yongin-si, Gyeonggi-do 446-712, Republic of Korea

ARTICLE INFO

Article history:
Received 13 January 2011
Accepted 21 September 2011
Available online 29 September 2011

ABSTRACT

Carbon nanotube (CNT) films are fabricated on indium tin oxide (ITO) glass substrates by combining electrophoresis with photolithography using ribonucleic acid (RNA)–CNT hybrids as functionalized CNTs and their emission properties are investigated. The CNTs are well-dispersed by wrapping them with RNA and well-defined RNA–CNT patterns are obtained on the ITO glass substrate. The RNA–CNT films show good field emission properties, such as high current densities, low turn-on fields, and uniform emission images. The RNA–CNT hybrids compare favorably to other functionalized CNTs for use in the electrophoretic deposition.

1. Introduction

CNTs as a form of carbon have attracted much attention in recent years because of their remarkable mechanical and electronic properties [1,2]. CNTs as field emitters have high aspect ratios and small radii of curvature, leading to significant enhancement of the electric-fields at their tips and resulting in low operating voltages for electron emission [1–3]. The CNTs are required to be patterned at selective positions with large-scale control for assembling and orientation. Previous methods for assembling and integrating CNTs on substrates include direct growth by chemical vapor deposition [4], screen-printing from a paste mixture of CNTs [5–7], self-assembling techniques [8], electrophoresis [9,10], and spraying [11,12] from a CNT solution. In particular, the electrophoresis is a high throughput and automated industrial process that has been widely used for coating colloidal particles, and has been recently applied to CNTs. The process enables efficient deposition of finely controlled film thickness and morphology. However, difficulties in this approach, specifically poor solubility of CNTs in most common solvents, and the tendency of CNTs to form large bundles, still hamper research efforts. A variety of different methods, such as liquid-phase dispersion with the aid of polymer wrapping [13], certain solvents [14], and surfactants [15,16], have been developed for exfoliation of the CNT. One area that shows particular promise is the dispersion of single-walled CNTs (SWCNTs) in water using deoxyribonucleic acid (DNA) or RNA [17,18]. SWCNTs have been dispersed in water using natural DNA and RNA, and custom-synthesized oligonucleotides. These dispersions have the advantage of using water, which is very safe and readily available, as a suspension. Here, we report the fabrication of uniform field emission cathodes by combining electrophoresis with photolithography using RNA–SWCNT hybrids as functionalized CNTs. Moreover, the emission properties of RNA–CNT films are investigated in terms of low and high purity SWCNTs.

2. Experimental

Low-purity SWCNTs (LSWCNTs), purchased from CarboLex Inc., are synthesized by the arc method, with a purity of about

* *Corresponding author:* Fax: +82 2 3290 3791.
E-mail address: bkju@korea.ac.kr (B.-K. Ju).
0008-6223/$ - see front matter
doi:10.1016/j.carbon.2011.09.043

60%. High-purity SWCNTs (HSWNTs) are synthesized by the high pressure CO conversion (HiPCO) method, obtained in purified form from Carbon Nanotechnologies Inc., with a purity of about 90%. The SWNTs have diameters between 1 and 2 nm, and were very long (at least 5 μm). RNA is a transfer RNA (tRNA) [19] from Baker's yeast, purchased from Sigma–Aldrich (Korea). The tRNA is a type of RNA with a small RNA chain of approximately 74–95 nucleotides. 80 mg of SWNT powder was mixed with 100 mL of deionized water and sonicated for 3 h by an ultra sonic homogenizer (20 kHz, 200 W). The SWCNT aqueous solution was mixed with a RNA aqueous solution, in which 40 mg of RNA was added to 100 mL of deionized water. The mixture was sonicated (40 Hz, 40 W) in an ice-water bath for 10 min and then centrifuged at 1800*g* for about 15 min. The HSWCNT aqueous solution was mixed with sodium dodecyl sulfate (SDS) aqueous solution, in which 240 mg of SDS was added to 100 mL of deionized water. The SDS–HSWCNT was sonicated (40 Hz, 40 W) in water bath for 2 h and then centrifuged at 1800*g* for about 15 min. In addition, 0.4 mL of TAE (4 mM Tris, 1.8 mM Acetic acid, 1 mM EDTA, pH 8) buffer solution were added to the prepared RNA–SWCNT and SDS–HSWCNT solution for stable electrophoresis.

Fig. 1 shows a schematic of the proposed electrophoretic deposition (see Fig. 1a) and SEM image of RNA–CNT hybrid film. In order to achieve a selective deposition, the substrate was conveniently patterned with photoresist (AZ 9260) by a photolithographic process. Since the RNA–CNT solution was water based, common photoresists can be use without concerns of photoresist dissolution during electrophoresis. A Pt plate and the masked ITO electrode were used as counter and working electrodes, respectively. Two electrodes were maintained at a distance of 1 cm. A constant dc voltage in the range of 5–10 V was applied to the electrodes for 3 min, resulting in selective deposition of RNA–SWCNT films on the ITO electrode that was applied to the positive bias. To leave only RNA–SWCNT films on the ITO electrode, the masked photoresist layer was removed with acetone. This sample was dried at 90 °C for 30 min in a conventional oven and then heated for 15 min by placing it in a furnace at a temperature of 380 °C, under a combination of air and N_2 environment. The diameter of the films, which was deposited in the shape of a dot (the number of dots: 196), was 400 μm and its patterns were well-defined as shown in Fig. 1b. The thickness of RNA treated LSWCNT and HSWCNT films are approximately 400 and 200 nm, respectively, as shown in Fig. S1 of Supporting Information (SI). The field emission properties of the fabricated cathodes were measured using a parallel plate geometry in a vacuum chamber under a pressure of more than 10^{-6} Torr. A variable dc voltage was applied between the cathode and anode separated by 240 μm. The anode was a glass substrate with an ITO coating, covered by a phosphor layer. The emission current was monitored by an electrometer and recorded at 1.0 s intervals. The emission images were taken by a digital camera. The prepared RNA–SWCNT solution was baked to dry and then observed using high resolution transmission electron microscopy (HRTEM, Technai G2 F30 of FEI Company). A scanning electron microscope (SEM, S-4800 of Hitachi Company) was also used to analyze the surface morphology.

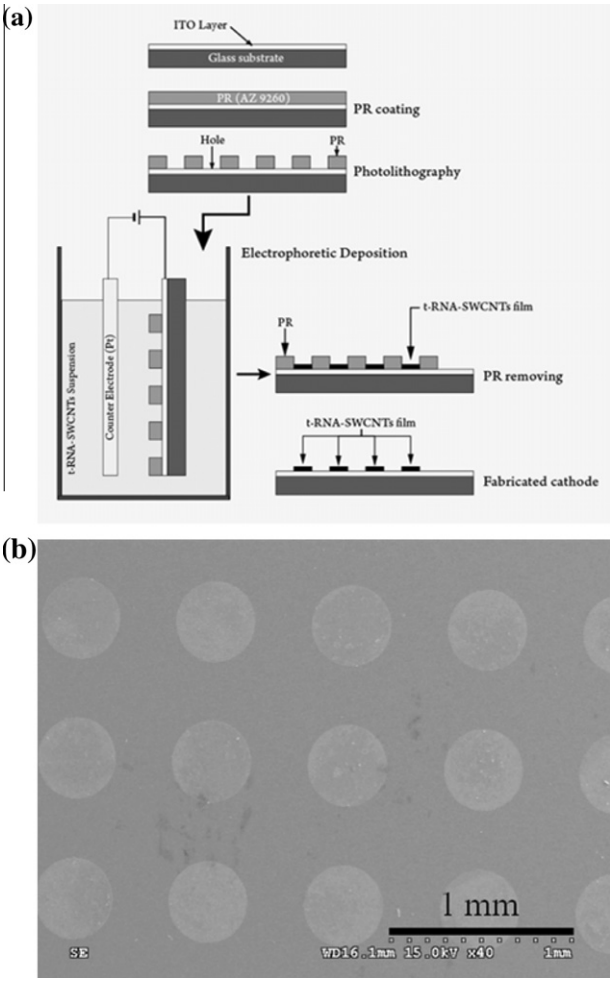

Fig. 1 – (a) Schematic fabrication process for the selective electrophoretic deposition of RNA–CNT hybrids on an ITO glass substrate and (b) SEM image of the patterns consist of RNA–CNT hybrids.

3. Results and discussion

Fig. 2 shows HRTEM images of RNA–LSWCNT and RNA–HSWCNT hybrids. The image in Fig. 2a shows the RNA coated around the SWCNTs and the contamination with amorphous carbon and metal catalyst. In contrast, amorphous carbon and metal catalyst appeared to be completely absent from the RNA-HSWNTs as shown in Fig. 2b. However, Fig. 2c and d shows an RNA chain wrapped helically around the LSWCNTs or the bundle HSWCNTs. The diameters of both the RNA–CNT hybrids were between 2 and 5 nm, indicating that most tubes are likely to be wrapped with only a RNA (diameter about 1–2 nm). Therefore, RNA–CNTs can be dispersed in deionized water to form a stable solution, regardless of impurities such as amorphous carbon and metal catalyst. The mechanism by which RNA acts to disperse can be explained in terms of the electrostatic properties of the RNA–SWCNT hybrids [20]. Although SWCNTs are electrically neutral, RNA carries a great deal of negative charges [19]. Thus, when individual nanotubes or small bundles of nanotubes are released by sonication, RNA binding through π-stacking

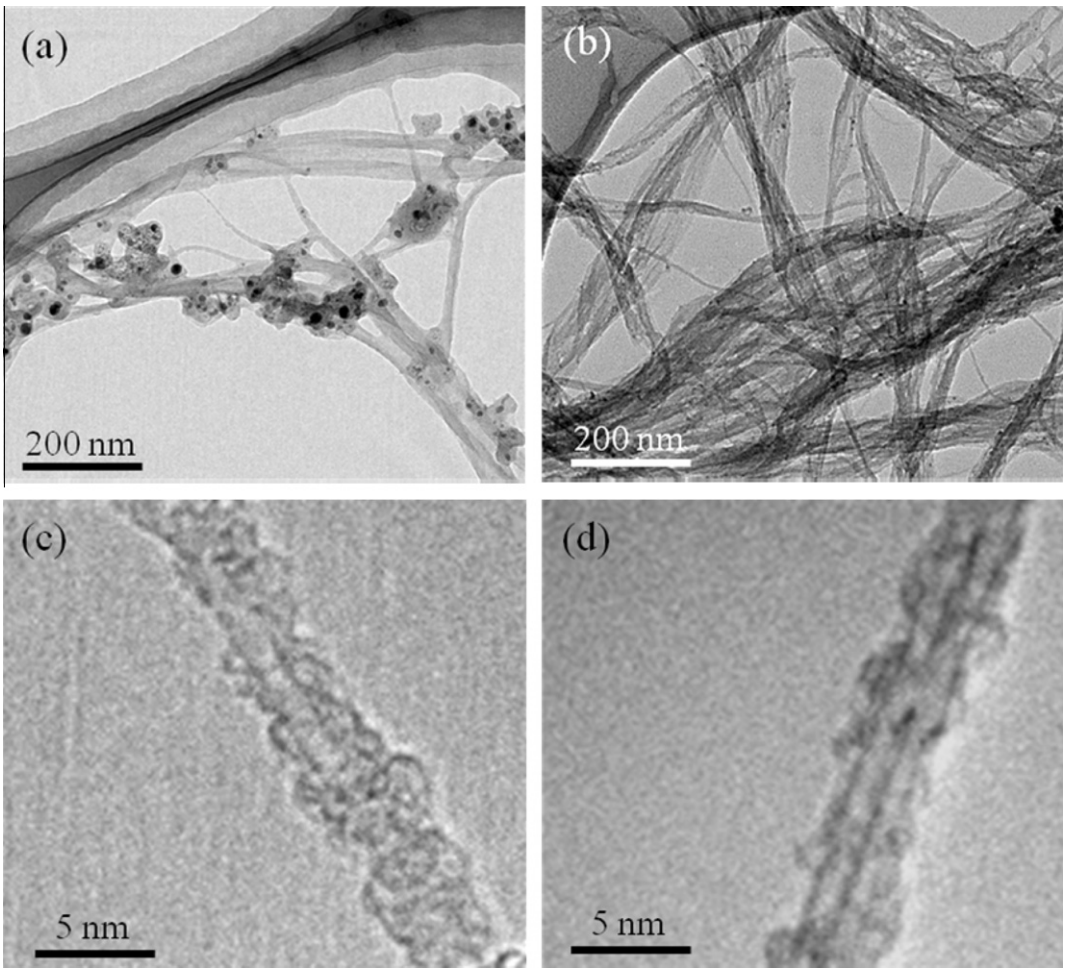

Fig. 2 – TEM Images of two RNA–SWCNT hybrids. The low magnification of (a) RNA–LSWCNT and (b) RNA–HSWCNT hybrids; the high magnification of (c) RNA–LSWCNT and (d) tRNA–HSWCNT hybrids.

creates a charge on them. As a result, rather than aggregating due to Van der Waals forces, the individual nanotubes or small bundles of nanotubes repel each other and form a stable solution.

Fig. 3 shows the FE-SEM images of the RNA–LSWCNT and RNA–HSWCNT films patterned on the ITO glass substrate before and after heat treatment at 380 °C in air and N_2. By heating at 380 °C, which is high enough to burn RNA and carbonaceous impurities but not high enough to burn the CNTs, a good deal of the extraneous material would be burnt off [12]. Each film was treated with an adhesive tape [21] for surface activation, which leads to preferential alignment along the vertical direction. Before heat treatment, the surface of the RNA–LSWCNT film included RNA–SWCNT hybrids and heavy contamination with amorphous carbon and metal catalyst (see Fig. 3a), but the surface of RNA–HSWCNT film contained only the RNA–SWCNT hybrids (see Fig. 3b). Because of this, the RNA–CNT hybrids in RNA–HSWCNT film were more uniformly distributed, than in the RNA–LSWCNT film over the pattern area. When samples were heated, the morphology of the RNA-HSCWNT film was almost unchanged (see Fig. 3d), and a lot of the CNTs or RNA–CNT hybrids still remained in the films which were aligned preferentially in the vertical direction (see Fig. 3f). In the case of the RNA–LSWCNT film, the surface morphology has changed dramatically (see Fig. 3c and e) and numerous, randomly distributed fissures have been created. Fig. 3e is a magnified image of a fissure in Fig. 3c. Where it can be seen that the CNTs protrude from the fissure. These may be RNA–CNTs or CNTs and most of them were cut. The fissures are probably formed by the shrinking and movement of composites consisting of RNA and impurities with amorphous carbon and metal catalyst in the film, due to the heat treatment.

Fig. 4a and b shows the measured field emission current densities as a function of the applied field and the corresponding Fowler–Nordheim (F–N) plots for each RNA–CNT film shown in Fig. 3. Samples A and B are selectively deposited on an ITO glass substrate using the RNA–LSWCNT and RNA–HSWCNT suspension, respectively. The current density was calculated by dividing the measured current by the total area of patterns, which is 0.246 cm^2. The field emission data were analyzed using the F–N model [22], and were replotted as ln (I/E^2) vs. 1/E (insets in Fig. 4a and b). The enhancement factor was derived from the slope of the graph by assuming that the work function of the CNTs was the same as the work function of graphite (~5 eV). Table 1 summarizes the turn-on

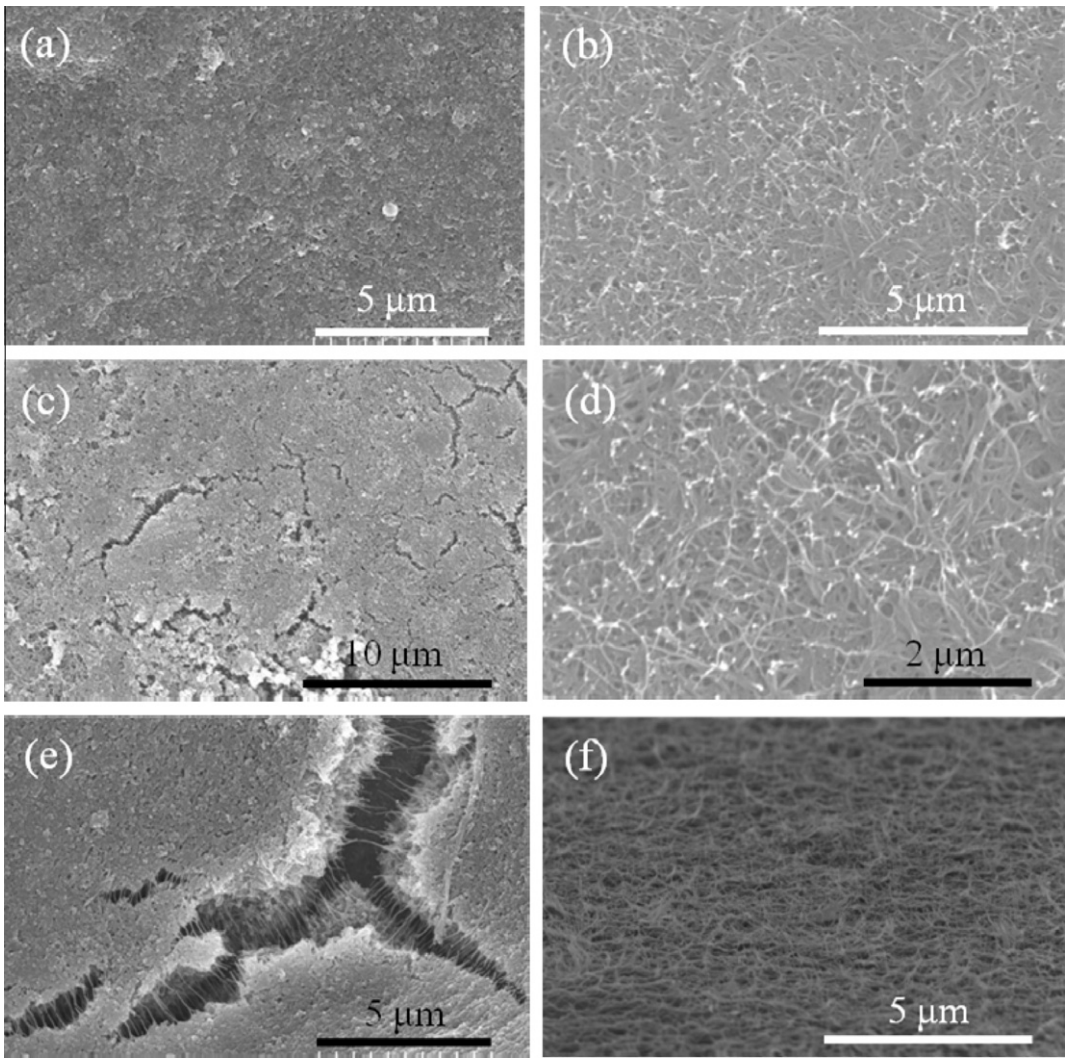

Fig. 3 – SEM images of the RNA–CNT films prepared on ITO glass substrates by the electrophoretic deposition using LSWCNTs and HSWCNTs based RNA–CNT suspension. In addition, all films were treated by adhesive tape as surface activation. (a) LSWCNT and (b) HSWCNT based RNA–CNT films before the heat treatment; (c) and (e) LSWCNTs and (d) and (f) HSWCNTs based RNA–CNT films after the heat treatment.

field for 100 μA/cm^2, the emission current density, and the field enhancement factor for the samples investigated. Samples, after the heat treatment, exhibited higher current densities and enhancement factors than those before heat treatment. The reason for this is different in each case; the results of sample A is due to the produced fissures in the film during the heat treatment (see Fig. 3c and e), whereas the result of sample B may be caused by improved activation through removing free RNA from the surface of the films by heating (see Fig. 3d and f).

In contrast, the turn-on field from sample A was similar to that from sample B under the same conditions. The overall emission sites of the samples are demonstrated in the order of sample B with the heat treatment > sample A with the heat treatment > sample B without the heat treatment > sample A without the heat treatment, as shown in Fig. 5. After the heat treatment, sample A showed a high current density and enhancement factor but the emission site of sample B was better than that of sample A because the produced fissures in sample A were non-uniformly and randomly distributed over the pattern as shown in Fig. 3c and e. Before the heat treatment, sample B, which showed the lower current density and enhancement factor relatively displayed the uniform emission image owing to the uniform distribution of RNA–CNT hybrids or CNTs over the pattern, as shown in Fig. 3d and f.

Fig. 6a shows the SEM image of the SDS–HSWCNT film. Turn-on field of SDS–HSWCNT film was 2.5 V/μm and current density was 4 mA/cm^2 by applying a field of 3.7 V/μm, as shown in Fig. 6b. The field emission image showed relatively better uniform sites for the RNA–CNT hybrid emitters compared to the SDS–CNT emitters. The RNA–CNT and SDS–CNT substrate were immersed in a beaker of acetone. The RNA–CNT hybrids were not removed. The adhesion of RNA–CNT hybrids on the ITO glass substrate is stronger than that of SDS–CNT on the ITO glass substrate. SDS–

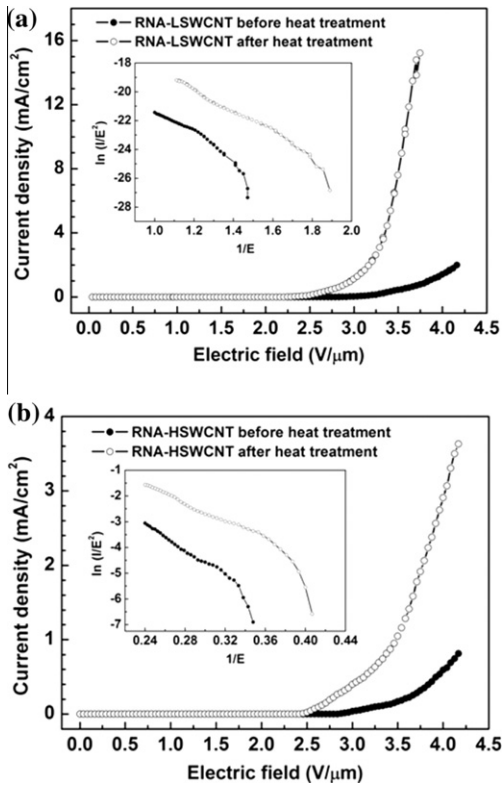

Fig. 4 – Current density vs. the applied electric field for (a) the RNA–LSWCNT film and (b) RNA–HSWCNT film before and after heat treatment. Inset is the F–N plots.

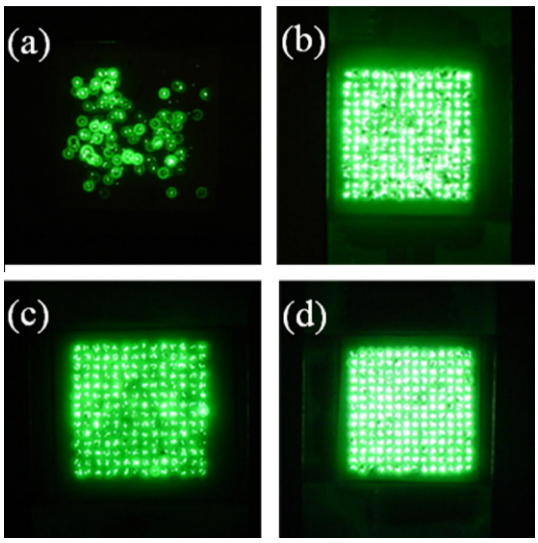

Fig. 5 – Field emission images of (a) RNA–LSWCNT and (b) RNA–HSWCNT films without the heat treatment, and (c) RNA–LSWCNT and (d) RNA–HSWCNT films with the heat treatment by applying a field of 4.1 V/μm.

CNT patterns were not well-defined when the masked photoresist layer was removed with acetone due to the poor surface adhesion between the SDS–CNT film and the substrate.

4. Conclusions

RNA–CNT films have been fabricated on ITO glass substrates by combining electrophoretic deposition with photolithography using two RNA–CNT suspensions based on the low and high purity SWNTs, and the field emission properties of each RNA–CNT film have been investigated. It has been found that CNTs are well-dispersed by wrapping them with RNA and RNA–CNT films are well-defined on the ITO layer, regardless of the purity of the CNTs used. From the heat treatment, it is found that the two RNA–CNT films have significantly enhanced the field emission properties, such as the current density, the enhancement factor, and uniform emission. The current density of the RNA–LSWCNT film is higher than that of the RNA–HSWCNT film. In the case of the emission site, the RNA–HSWCNT film shows better results than the RNA–LSWCNT film. Overall, RNA–CNT hybrids could be made into a micro-patterned film with high resolution, and applied to field emission devices for high currents, such as X-ray and electric beam sources, and for uniform emission images such as displays, lamps, and back light unit.

Acknowledgments

This work was supported by the Industrial Core Technology Development Program funded by the Ministry of Knowledge Economy (No. 10037394), Seoul Metropolitan Government though Seoul Research and Business Development (Grant No. CR070054), World Class University (WCU, R32-2009-000-10082-0) Project of the Ministry of Education, Science and Technology (Korea Science and Engineering Foundation), Samsung Advanced Institute of Technology, and Korea University Grant. We also like to thank the Korea Basic Science Institute for the use of TEM.

Table 1 – Turn-on field, emission current density and enhancement factor values for LSWCNT and HSWCNT based RNA–CNT films before and after the heat treatment.

Sample type		Turn-on field for 100 μA/cm² (V/μm)	Current density at 3.7 V/μm (mA/cm²)	Enhancement factor β
RNA–LSWCNT films (sample A)	Before heat treatment	3.58	0.17	6356
	After heat treatment	2.49	15.21	9258
RNA–HSWCNT films (sample B)	Before heat treatment	3.25	0.31	2669
	After heat treatment	2.62	1.91	3514

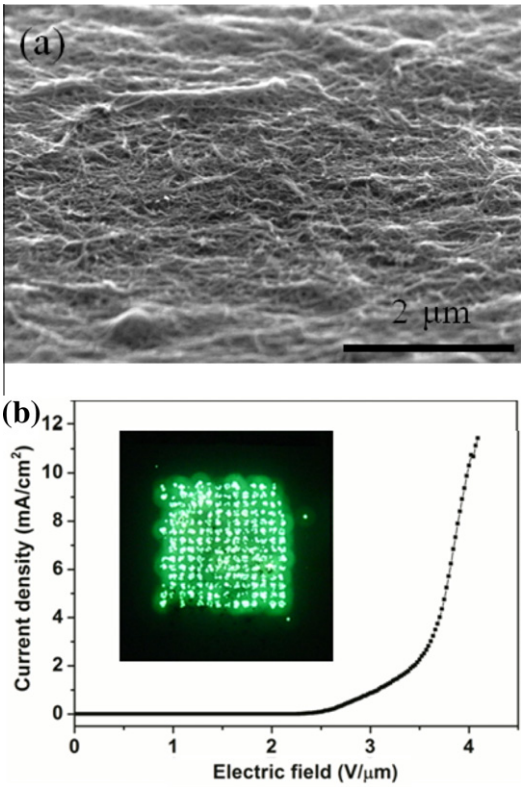

Fig. 6 – (a) SEM image of the SDS–HSWCNT film prepared on ITO glass substrate by the electrophoretic deposition. (b) Current density vs. applied electric field for the SDS–HSWCNT film. Inset is the field emission image of SDS–HSWCNT by applying a field of 4.1 V/μm.

Appendix A. Supplementary data

Supplementary data associated with this article can be found, in the online version, at doi:10.1016/j.carbon.2011.09.043.

REFERENCES

[1] Ajayan PM. Nanotubes from carbon. Chem Rev 1999;99(7):1787–800.
[2] Rao CNR, Satishkumar BC, Govindaraj A, Nath M. Nanotube. Chem Phys Chem 2001;2(2):78–105.
[3] Baughman RH, Zakhidov AA, de Heer WA. Carbon nanotube – the route toward applications. Science 2002;297(5582):787–92.
[4] Sohn JI, Lee SH, Song JH, Choi SY, Cho KI, Nam KS. Patterned selective growth of carbon nanotubes and large field emission from vertically well-aligned carbon nanotube field emitter arrays. Appl Phys Lett 2001;78(7):901–3.
[5] Kim YC, Nam JW, Hwang MI, Kim IH, Lee CS, Choi YC, et al. Uniform and stable field emission from printed carbon nanotubes through oxygen trimming. Appl Phys Lett. 2008;92(26):263112-1–3.
[6] Lee HJ, Lee YD, Cho WS, Lee YH, Han JH, Kim JK, et al. Field emission enhancement from change of printed nanotube morphology by an elastomer. Appl Phys Lett 2006;88(9):0931151–931153.
[7] Wang QH, Setlur AA, Lauerhaas JM, Dai JY, Seelig EW, Chang RPH. A nanotube-based field emission flat panel display. Appl Phys Lett 1998;72(22):2912–3.
[8] Oh SJ, Cheng Y, Zhang J, Shimoda H, Zhou O. Room-temperature fabrication of high-resolution carbon nanotube field-emission cathodes by self-assembly. Appl Phys Lett 2003;82(15):2521–3.
[9] Jung SM, Jung HY, Suh JS. Horizontally aligned carbon nanotube field emitters fabricated on ITO glass substrates. Carbon 2008;46(14):1973–7.
[10] Boccaccini AR, Cho J, Roether JA, Thomas BJC, Minay EJ, Shaffer MSP. Electrophoretic deposition of carbon nanotubes. Carbon 2006;44(15):3149–60.
[11] Jeong HJ, Choi HK, Kim GY, Song YI, Tong Y, Lim SC, et al. Fabrication of efficient field emitters with thin multiwalled carbon nanotubes using spray method. Carbon 2006;44(13):2689–93.
[12] Cho WS, Lee YD, Kim YC, Son YC, Heo JN, Han IT, et al. Fabrication and field emission properties of spray-deposited RNA–carbon nanotube films. Electrochem Solid State Lett 2009;12(9):J83–6.
[13] Manchado MAL, Valentini L, Biagiotti J, Kenny JM. Thermal and mechanical properties of single-walled carbon nanotubes–polypropylene composites prepared by melt processing. Carbon 2005;43(7):1499–505.
[14] Bergin SD, Nicolosi V, Giordani S, de Gromard A, Carpenter L, Blau WJ, et al. Exfoliation in ecstasy: liquid crystal formation and concentration-dependent debundling observed for single-wall nanotubes dispersed in the liquid drug ð -butyrolactone. Nanotechnology 2007;18(45):4557051–45570510.
[15] Bergin SD, Nicolosi V, Cathcart H, Lotya M, Rickard D, Sun Z, et al. Large populations of individual nanotubes in surfactant-based dispersions without the need for unltracentrifugation. J Phys Chem C 2008;112(4):972–7.
[16] Bachilo SM, Strano MS, Kittrell C, Hauge RH, Smalley RE, Weisman RB. Structure-assigned optical spectra of single-walled carbon nanotubes. Science 2002;298(5602):2361–6.
[17] Cathcart H, Nicolosi V, Hughes JM, Blau WJ, Kelly JM, Quinn SJ, et al. Ordered DNA wrapping switches on luminescence in single-walled nanotube dispersions. J Am Chem Soc 2008;130(38):12734–44.
[18] Jeynes JCG, Mendoza E, Chow DCS, Watts PCP, McFadden J, Silva SRP, et al. Generation of chemically unmodified pure single-walled carbon nanotubes by solubilizing with RNA and treatment with ribonuclease A. Adv. Mater 2006;18(12):1598–602.
[19] Saeger, W, Principles of nucleic acid structure, NewYork: Springer-Verlag, p. 184.
[20] Johnson RR, Johnson ATC, Klein ML. Probing the structure of DNA–carbon nanotube hybrids with molecular dynamics. Nano Lett 2008;8(1):69–75.
[21] Vink TJ, Cillies M, Kriege JC, van de Laar HWJJ. Enhanced field emission from printed carbon nanotubes by mechanical surface modification. Appl Phys Lett 2003;83(17):3552–4.
[22] Fowler RH, Nordheim LW. Proc Roy Soc London A 1928;119:173–81.